

Investigation of Cryogenic Current-Voltage Anomalies in SiGe HBTs: Role of Base-Emitter Junction Inhomogeneities

Nachiket R. Naik ¹, Bekari Gabritchidze ², Jacob Kooi ³, Kieran A. Cleary ² and Austin J. Minnich ^{1,*}

¹*Division of Engineering and Applied Science,*

California Institute of Technology, Pasadena, CA 91125

²*Cahill Radio Astronomy Lab , California Institute of Technology, Pasadena, CA 91125*

³*NASA Jet Propulsion Laboratory, California Institute of Technology, Pasadena, CA 91109*

(Dated: March 1, 2023)

Abstract

The anomalous current-voltage characteristics of cryogenic SiGe HBTs have been a topic of investigation for many years. Proposed explanations include quasiballistic transport of electrons across the base or tunneling from the emitter to the collector, but inconsistencies exist with these hypotheses. Although similar behavior occurs in Schottky junctions and has been attributed to lateral inhomogeneities in the junction potential, this explanation has not been considered for SiGe HBTs. Here, we experimentally investigate this hypothesis by characterizing the base-emitter built-in potential and its temperature dependence using both capacitance-voltage and current-voltage characteristics. We observe a marked discrepancy in the built-in potential obtained using these two methods at cryogenic temperatures, supporting the origin for the anomalous behavior of SiGe HBTs as arising from lateral inhomogeneities in the base-emitter junction potential. This work helps to identify the physical mechanisms limiting the cryogenic microwave noise performance of SiGe HBTs.

* aminnich@caltech.edu.

I. INTRODUCTION:

Silicon-germanium heterojunction bipolar transistors (HBTs) are widely used in microwave applications such as high-speed communications and radar systems owing to their competitive microwave performance, low cost, and ease of integration compared with III-V compound semiconductor devices [1]. Technological advances such as reduced emitter widths, decreased base resistances and extrinsic capacitances, and advanced epitaxial techniques have enabled RF performance rivaling that of III-V high electron mobility transistors [2, 3]. Recently, owing to these strengths, cryogenic SiGe HBTs have been considered for applications in quantum computing and radio astronomy [4, 5].

The cryogenic microwave performance of SiGe HBTs has been investigated following their initial development in the late 1980s [6] as various performance metrics such as transconductance and noise figure improve with cooling. However, below ~ 77 K, these improvements are observed to plateau with decreasing temperature [7, 8], corresponding to a temperature-dependent ideality factor $n(T)$ that greatly exceeds unity at cryogenic temperatures [9, 10]. This behavior differs markedly from the predictions of thermionic emission theory of an ideal junction in which n is equal to unity and is independent of temperature, and the transconductance increases inversely with temperature. [11, 12].

This cryogenic non-ideal behavior has been attributed to various mechanisms including quasiballistic transport [8, 13], direct tunneling [9], or trap-assisted tunneling [14]. However, a recent theory work has reported that quasiballistic electron transport cannot explain the observed collector cryogenic non-idealities [15]. Further, these non-idealities have been observed in devices with base widths of ~ 100 nm [5] for which direct tunneling is negligible. As a result, the origin of these cryogenic anomalies remains a topic of investigation.

In a different context, similar anomalies have been observed and extensively investigated in Schottky diodes [11, 16, 17], and they were ultimately attributed to lateral inhomogeneities in the built-in potential Φ_{BI} . [18] It was shown through numerical simulations [19] and experiments [11, 18] that different spatial distributions of barrier inhomogeneities yielded different trends of ideality factor versus temperature, with some that are similar to those seen in HBTs at cryogenic temperatures [18, Fig. 15]. The experimental evidence for this effect is the discrepancy between the built-in potentials extracted from capacitance-voltage (CV) characteristics versus those from IV characteristics at cryogenic temperatures because the

IV characteristics vary exponentially with the barrier height whereas the CV characteristics vary with a weaker polynomial dependence. [17]. However, whether this explanation is also applicable to HBTs has not been considered.

Here, we experimentally investigate this possibility by characterizing the base-emitter built-in potential using IV and CV measurements in modern SiGe HBTs at cryogenic temperatures. We observe a marked discrepancy between Φ_{BI} extracted from these methods, consistent with presence of lateral inhomogeneities in the base-emitter junction potential. We suggest a possible physical origin of the inhomogeneities as Ge clusters or electrically active C impurities which are introduced to minimize dopant diffusion. Our work advances efforts to improve the cryogenic microwave noise performance of SiGe HBTs.

II. THEORY AND METHODS:

A. Overview

Spatial inhomogeneities in the base-emitter potential may be identified by a discrepancy in built-in potential as measured from IV and CV characteristics due to the difference in their functional dependence on Φ_{BI} . In more detail, the collector current I_C is given by the diode equation:

$$I_C = A \exp(-q\Phi_{BI}/kT) \exp(qV_{BE}/n(T)kT) \quad (1)$$

where A is a constant prefactor, V_{BE} is the base-emitter voltage, and $n(T)$ is the ideality factor. The ideality factor may also be reported as an effective temperature $T_{eff} = n(T)T_{phys}$ [8]. The temperature dependence of Φ_{BI} , relative to a value at a reference temperature, can be obtained by fitting the ideal portion of the $I_C - V_{BE}$ characteristics with (1) and neglecting any temperature-dependence of A . $n(T)$ can also be extracted from the slope of the IV Gummel curves. Variations in Φ_{BI} over the emitter area can lead to $n(T) \gg 1$, particularly at cryogenic temperatures due to the $1/T$ dependence in the exponential as seen in (1).

The capacitance-voltage characteristics of the base-emitter junction may also be used to obtain the built-in potential. The base-emitter depletion capacitance C_{BE} is given by [12]

$$C_{BE}(V_{BE}) = \frac{C_{BE,0}}{\left(1 - \frac{V_{BE}}{\Phi_{BI}}\right)^m} \quad (2)$$

where $C_{BE,0}$ is the zero-bias junction capacitance and m is a characteristic exponent. For a uniformly doped junction, $m = 1/2$. As is evident from (2), C_{BE} varies with Φ_{BI} much less strongly compared to (1), and therefore C_{BE} is less sensitive to spatial inhomogeneities relative to $I_C - V_{BE}$ characteristics. Discrepancies between the Φ_{BI} extracted using these two methods are therefore interpreted as evidence for the presence of inhomogeneities in the junction potential.

B. Experimental methods

We extracted Φ_{BI} from $C_{BE} - V_{BE}$ and $I_C - V_{BE}$ characteristics from 20 – 300 K on a SiGe HBT (SG13G3, IHP). The discrete transistors were probed in a custom-built cryogenic probe station. [20, 21] We employed Nickel/Tungsten probes (40A-GSG-100-DP, GGB Industries) which are suitable for probing Al pads. $I_C - V_{BE}$ characteristics are performed at a constant collector voltage $V_{CE} = 1$ V. Φ_{BI} is extracted relative to its value at a reference temperature from the intercept of a linear fit of $\ln(I_C)$ versus V_{BE} from (1), and $n(T)$ is extracted from the slope of this fit.

Following standard procedure [10, 11] $C_{BE} - V_{BE}$ characteristics are obtained using a vector network analyzer (VNA, Keysight E5061B). In reverse-bias and low-forward bias regimes, the Y -parameters are given by $Y_{11} = g_{BE} + j\omega(C_{BE} + C_{BC})$ and $Y_{12} = -j\omega C_{BC}$, where C_{BC} is the base-collector depletion capacitance. The base-emitter capacitance can therefore be expressed as $C_{BE} = (\text{Im}(Y_{11} + Y_{12}))/2\pi f$. V_{BE} is restricted to [-0.5 V, +0.5 V] to minimize the contributions of the conductance and diffusion capacitance. $V_{BC} = 0$ V is held constant to ensure C_{BC} is constant while V_{BE} is swept. The Y parameters are measured in 1 – 3 GHz, and the extractions are performed at 2.4 GHz. At these frequencies, it is observed that the imaginary part of Y_{11} is linear in frequency, indicating purely capacitive behavior. SOLT calibration is performed on a CS-5 calibration standard at each temperature, and the shunt parasitic capacitance at the input of the device is de-embedded using an OPEN structure. The intermediate-frequency bandwidth (1 kHz) and frequency points (every 0.2 GHz) are selected to limit the total sweep time to less than 15 s to avoid drift. At each bias, Y -parameters are swept across frequency and ensemble-averaged 10 times. Φ_{BI} is extracted

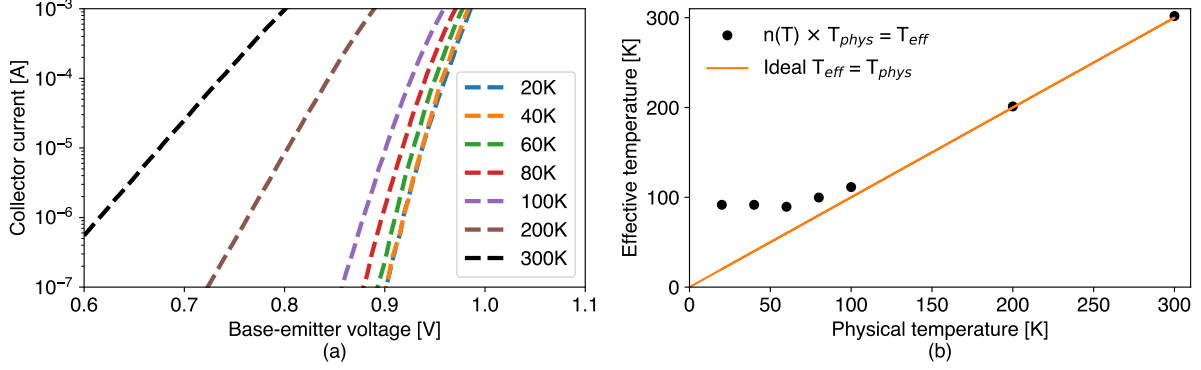


FIG. 1: (a) Measured I_C versus V_{BE} for various temperatures. The characteristics become independent of temperature at cryogenic temperatures. (b) $T_{eff} = n(T)T_{phys}$ vs T_{phys} from measurements (symbols) and theory (line), indicating the non-ideality of the base-emitter junction at cryogenic temperatures.

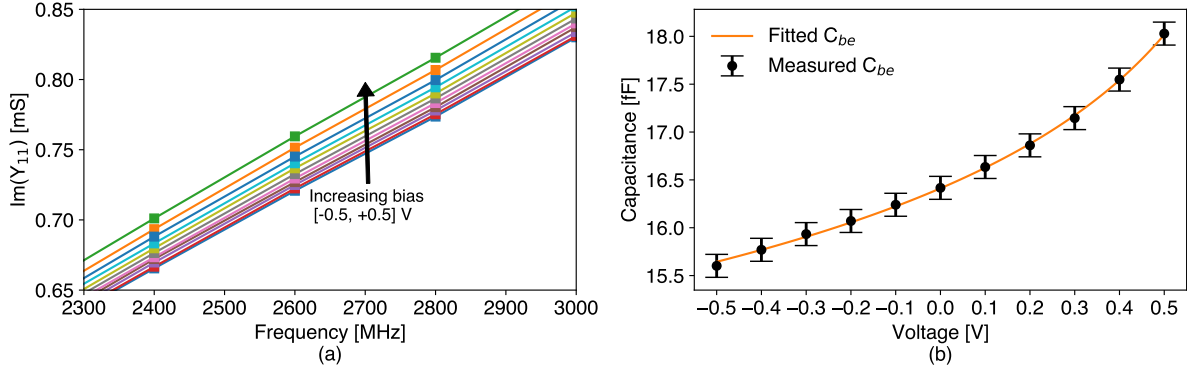


FIG. 2: (a) $Im(Y_{11})$ versus f at 300 K for various V_{BE} in steps of 0.1 V. The linear trend in frequency confirms purely capacitance behavior within the frequency and bias range. (b) Measured and fitted C_{BE} versus V_{BE} at 300 K. The fit yields $\Phi_{BI} = 0.83$ V and $m = 0.10$.

from a sweep of C_{BE} versus V_{BE} by fitting the parameters Φ_{BI} , $C_{BE,0}$ and m as in (2) using a trust region reflective (TRF) algorithm from the SciPy library. [22] Φ_{BI} is constrained to [0.5 V, 1.2 V], $C_{BE,0}$ is constrained between the minimum and maximum values of the sweep, and m is constrained to [0, 1].

III. RESULTS

Fig. 1a shows the collector current I_C versus V_{BE} at various temperatures between 20 K and 300 K. Consistent with prior findings, [5, 8, 9] the measurements exhibit deviations from (1) at cryogenic temperatures, with the curves exhibiting a weakening dependence on temperature below ~ 80 K. $n(T)$ at each physical temperature is extracted from the slope obtained by fitting a line to each curve in Fig. 1a. The current range used for this fitting is limited to 0.2 mA to exclude effects of series resistance. We plot the extracted $n(T)$ as $T_{eff} = n(T)T_{phys}$ versus T_{phys} in Fig. 1b. T_{eff} is observed to deviate from the ideal predictions of (1), saturating to ~ 100 K due to $n(T) > 1$ at cryogenic temperatures as has been reported previously [8].

We next examine the RF characteristics. Fig. 2a plots $Im(Y_{11})$ versus f for various V_{BE} at 300 K. A narrowed frequency range from the 1 – 3 GHz measurements is plotted to distinguish the curves. From these data and those for $Im(Y_{12})$, the de-embedded base-emitter capacitance C_{BE} is obtained. Fig. 2b plots the resulting C_{BE} versus V_{BE} at 300 K along with the fitted curve from (2). The error bars, representing the 2σ error in C_{BE} , are obtained from the 10 $C - V$ sweeps performed at each temperature.

Following the discussion in Sec. II, these data are analyzed to obtain Φ_{BI} from the $I_C - V_{BE}$ and $C_{BE} - V_{BE}$ characteristics. At room temperature, $\Phi_{BI}(CV)$ is found to be 0.83 V, in good agreement with [10]. This value is specified as the room temperature value for $\Phi_{BI}(IV)$ to facilitate comparison at other temperatures. Fig. 3 plots the Φ_{BI} from both measurements versus T_{phys} . For $\Phi_{BI}(CV)$, the error bars represent the $2\text{-}\sigma$ error in Φ_{BI} , obtained by performing fits with (2) for 100 $C_{BE} - V_{BE}$ sweeps with errors randomly determined based on a normal distribution defined by the uncertainty in the measured C_{BE} . The extracted $\Phi_{BI}(CV)$ is observed to weakly increase with decreasing temperature, consistent with observations for similar devices [10] and Schottky diodes [17]. In contrast, $\Phi_{BI}(IV)$ exhibits a stronger dependence on temperature, as observed previously for Schottky diodes [11, 17], and differs markedly in magnitude from the $\Phi_{BI}(CV)$. Following a method employed in the Schottky junction literature, [17] we also plot $\Phi_{BI}(IV)n(T)$, which for Schottky junctions has been empirically observed to agree with the measured $\Phi_{BI}(CV)$. This effect is also observed in the present data for the SiGe base-emitter junction.

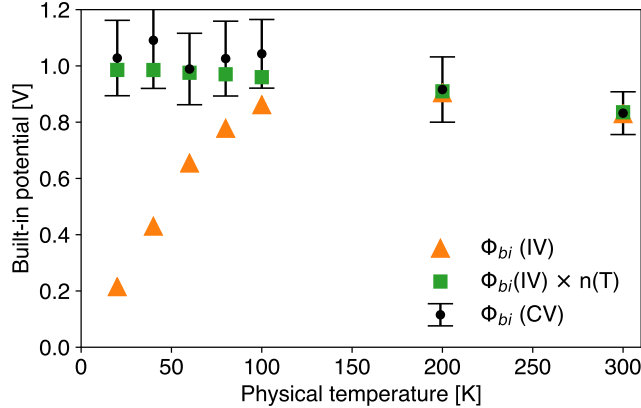


FIG. 3: Built-in potential Φ_{BI} versus physical temperature from *CV* and *IV* data. Also plotted is the empirical relation $\Phi_{BI}(IV)n(T)$ from the Schottky junction literature. The measured $\Phi_{BI}(CV)$ agrees well with this quantity, supporting the existence of lateral spatial inhomogeneities in Φ_{BI} .

IV. DISCUSSION:

We have shown that the cryogenic current anomalies in SiGe HBTs exhibit features that are qualitatively similar to those observed previously in Schottky junctions. The similarity of the base-emitter junction characteristics with those reported for Schottky junctions provides evidence for the similarity of the underlying physical mechanism, inhomogeneities in Φ_{BI} across the emitter area. In Schottky junctions, techniques such as ballistic emission electron microscopy have enabled the barrier-potential variation to be linked to specific material defects such as dislocations. [11] We now discuss material defect origins of the base-emitter junction potential inhomogeneities in HBTs. Prior modeling studies of Schottky junctions have found that variations in barrier potential on the scale of the space-charge region (SCR) width can result in $n(T) \gg 1$ at cryogenic temperatures. [18, 19] Such variations in potential have been postulated to occur in SiGe HBTs and other SiGe films grown by chemical vapor deposition due to clustering of Ge [23] or electrically active carbon defects [24]. Non-uniformities in Ge content over a few nanometers in SiGe p-wells with mean Ge content exceeding 30% have been shown to negatively affect electrical properties like hole mobility [23]. With Ge concentrations in modern SiGe HBTs being on the order of 30% [9], Ge clusters are a conceivable origin of the barrier potential inhomogeneity. Studies of

low-frequency noise in HBTs have also found evidence for trap states associated with C impurities, [24] which are present in modern HBTs in concentrations on the order of 10^{20} cm^{-3} . [1] The precise origin of the inhomogeneities in terms of materials defects will require a thorough characterization of the structural and electrical properties of carefully prepared SiGe heterojunctions.

Finally, we discuss the possible improvements in microwave amplification and noise performance that may be obtained with more ideal base-emitter junctions. A more homogeneous base-emitter junction potential will result in cryogenic transconductance and collector current values which are closer to their ideal values. Further, improved ideality in these DC parameters directly affects the minimum noise temperature T_{min} of HBTs. For example, a decrease in T_{eff} from 80 K to the physical temperature 20 K, corresponding to an ideality factor at 20 K of $n = 1$ instead of $n = 4$, linearly improves the achievable T_{min} by a factor of 4 in the low-frequency and low base-resistance limit (see Eqn. (2) in Ref. [4]). Therefore, minimizing inhomogeneities in the base-emitter junction potential is expected to lead to improved cryogenic microwave noise performance, advancing their application in quantum science and engineering.

V. CONCLUSION:

We have reported measurements of the built-in potential of the base-emitter junction and its temperature dependence of a SiGe HBT using IV and CV characteristics. The differing values of the built-in potential at cryogenic temperatures obtained from these two methods supports the origin of cryogenic electrical anomalies as arising from lateral inhomogeneities in the base-emitter junction potential. The physical origin of these barrier inhomogeneities is hypothesized to be Ge clustering or C impurities. This work advances efforts to improve the cryogenic microwave noise performance of SiGe HBTs.

ACKNOWLEDGMENTS

The authors thank Sander Weinreb, Pekka Kangaslahti, Akim Babenko, Holger Rucker, Nicolas Derrier, John Cressler, and Xiaodi Jin for useful discussions. This work was supported by NSF Award Number 1911926 and by JPL PDRDF Project Number 107978.

AUTHOR DECLARATIONS

Conflict of Interest

The authors have no conflicts to disclose.

DATA AVAILABILITY

The data that support the findings of this study are available from the corresponding author upon reasonable request.

-
- [1] J. D. Cressler and G. Niu, *Silicon-germanium heterojunction bipolar transistors* (Artech house, 2003).
 - [2] P. Chevalier, M. Schroter, C. R. Bolognesi, V. D'Alessandro, M. Alexandrova, J. Bock, R. Flickiger, S. Fregonese, B. Heinemann, C. Jungemann, R. Lovblom, C. Maneux, O. Ostinelli, A. Pawlak, N. Rinaldi, H. Rucker, G. Wedel, and T. Zimmer, Si/SiGe:C and InP/GaAsSb Heterojunction Bipolar Transistors for THz Applications, [Proceedings of the IEEE](#) **105**, 1035 (2017).
 - [3] W. T. Wong, M. Hosseini, H. Rucker, and J. C. Bardin, A 1 mW cryogenic LNA exploiting optimized SiGe HBTs to achieve an average noise temperature of 3.2 K from 4-8 GHz, in [IEEE MTT-S International Microwave Symposium Digest](#), Vol. 2020-Augus (Institute of Electrical and Electronics Engineers Inc., 2020) pp. 181–184.
 - [4] J. C. Bardin, S. Montazeri, and S. W. Chang, Silicon Germanium Cryogenic Low Noise Amplifiers, *Journal of Physics: Conference Series* **834**, [10.1088/1742-6596/834/1/012007](https://doi.org/10.1088/1742-6596/834/1/012007) (2017).
 - [5] H. Ying, J. Dark, A. P. Omprakash, B. R. Wier, L. Ge, U. Raghunathan, N. E. Lourenco, Z. E. Fleetwood, M. Mourigal, D. Davidovic, and J. D. Cressler, Collector Transport in SiGe HBTs Operating at Cryogenic Temperatures, [IEEE Transactions on Electron Devices](#) **65**, 3697 (2018).
 - [6] G. L. Patton, S. S. Iyer, S. L. Delage, S. Tiwari, and J. M. Stork, Silicon-Germanium-Base Heterojunction Bipolar Transistors By Molecular Beam Epitaxy, [IEEE Electron Device Letters](#) **9**, 165 (1988).

- [7] A. J. Joseph, J. D. Cressler, and D. M. Richey, Operation of SiGe Heterojunction Bipolar Transistors in the Liquid-Helium Temperature Regime, [IEEE Electron Device Letters](#) **16**, 268 (1995).
- [8] J. C. Bardin, *Silicon-Germanium Heterojunction Bipolar Transistors For Extremely Low-Noise Applications*, Ph.D. thesis, California Institute of Technology (2009).
- [9] H. Rucker, J. Korn, and J. Schmidt, Operation of SiGe HBTs at cryogenic temperatures, [Proceedings of the IEEE Bipolar/BiCMOS Circuits and Technology Meeting](#) , 17 (2017).
- [10] X. Jin, M. Muller, P. Sakalas, A. Mukherjee, Y. Zhang, and M. Schroter, Advanced SiGe:C HBTs at Cryogenic Temperatures and Their Compact Modeling with Temperature Scaling, [IEEE Journal on Exploratory Solid-State Computational Devices and Circuits](#) **7**, 175 (2021).
- [11] W. Mönch, *Semiconductor Interfaces* (Springer, Berlin, Heidelberg, 2001) pp. 385–481.
- [12] S. M. Sze, Y. Li, and K. K. Ng, *Physics of semiconductor devices* (John wiley & sons, 2021).
- [13] D. M. Richey, A. J. Joseph, J. D. Cressler, and R. C. Jaeger, Evidence for non-equilibrium base transport in Si and SiGe bipolar transistors at cryogenic temperatures, *Solid-State Electronics* **39**, 785 (1996).
- [14] D. Davidović, H. Ying, J. Dark, B. R. Wier, L. Ge, N. E. Lourenco, A. P. Omprakash, M. Mourigal, and J. D. Cressler, Tunneling, current gain, and transconductance in silicon-germanium heterojunction bipolar transistors operating at millikelvin temperatures, [Physical Review Applied](#) **8**, 1 (2017).
- [15] N. R. Naik and A. J. Minnich, Quasiballistic electron transport in cryogenic SiGe HBTs studied using an exact, semi-analytic solution to the Boltzmann equation, [Journal of Applied Physics](#) **130**, 174504 (2021).
- [16] R. Hackam and P. Harrop, Electrical Properties of Nickel-Low-Doped n-Type Gallium Arsenide Schottky-Barrier Diodes, [IEEE Transactions on Electron Devices](#) **19**, 1231 (1972).
- [17] A. S. Bhuiyan, A. Martinez, and D. Esteve, A new Richardson plot for non-ideal schottky diodes, [Thin Solid Films](#) **161**, 93 (1988).
- [18] R. T. Tung, Electron transport at metal-semiconductor interfaces: General theory, [Physical Review B](#) **45**, 13509 (1992).
- [19] J. P. Sullivan, R. T. Tung, M. R. Pinto, and W. R. Graham, Electron transport of inhomogeneous Schottky barriers: A numerical study, [Journal of Applied Physics](#) **58**, 7403 (1991).

- [20] B. Gabritchidze, K. Cleary, J. Kooi, I. Esho, A. C. Readhead, and A. J. Minnich, Experimental characterization of temperature-dependent microwave noise of discrete hemts: Drain noise and real-space transfer (IEEE, 2022) pp. 615–618.
- [21] D. Russell, K. Cleary, and R. Reeves, Cryogenic probe station for on-wafer characterization of electrical devices, [Review of Scientific Instruments](#) **83**, 044703 (2012).
- [22] P. Virtanen, R. Gommers, T. E. Oliphant, M. Haberland, T. Reddy, D. Cournapeau, E. Burovski, P. Peterson, W. Weckesser, J. Bright, S. J. van der Walt, M. Brett, J. Wilson, K. J. Millman, N. Mayorov, A. R. J. Nelson, E. Jones, R. Kern, E. Larson, C. J. Carey, Í. Polat, Y. Feng, E. W. Moore, J. VanderPlas, D. Laxalde, J. Perktold, R. Cimrman, I. Henriksen, E. A. Quintero, C. R. Harris, A. M. Archibald, A. H. Ribeiro, F. Pedregosa, P. van Mulbregt, and SciPy 1.0 Contributors, SciPy 1.0: Fundamental Algorithms for Scientific Computing in Python, [Nature Methods](#) **17**, 261 (2020).
- [23] R. A. Kiehl, P. E. Batson, J. O. Chu, D. C. Edelstein, F. F. Fang, B. Laikhtman, D. R. Lombardi, W. T. Masselink, B. S. Meyerson, J. J. Nocera, A. H. Parsons, C. L. Stanis, and J. C. Tsang, Electrical and physical properties of high-Ge-content Si/SiGe p-type quantum wells, [Physical Review B](#) **48**, 11946 (1993).
- [24] J. Raoult, F. Pascal, C. Delseny, M. Marin, and M. J. Deen, Impact of carbon concentration on 1f noise and random telegraph signal noise in SiGe:C heterojunction bipolar transistors, [Journal of Applied Physics](#) **103**, 10.1063/1.2939252 (2008).